Fourth International Conference on FRP Composites in Civil Engineering (CICE2008)
22-24July 2008, Zurich, Switzerland

Modeling of thermo-mechanical properties and responses for FRP composites in fire

Y. Bai, T. Keller & T. Vallée

Composite Construction Laboratory, (CCLab), Ecole Polytechnique Fédérale de Lausanne, (EPFL), Station 16, Bâtiment BP, CH-1015 Lausanne, Switzerland

ABSTRACT: The changes of mechanical properties of FRP composites subjected to elevated and high temperatures were modeled based on chemical kinetic theory; they compared well with experimental results obtained by Dynamic Mechanical Analysis (DMA). Together with the material property sub-models, a thermo-mechanical model was then developed to predict the thermal and mechanical responses (temperature and elastic deflection) of full-scale cellular FRP panels subjected to a four-point bending configuration and fire from one side. Two different thermal boundary conditions were investigated: with and without liquid-cooling of the panels in the cells. Finite difference method was used to calculate the temperature, E-modulus and effective coefficient of thermal expansion in time and space domain. The elastic deflection due to stiffness degradation and thermal expansion were obtained at each time step based on classical beam theory. The predicted results compared well with the measured data over a test period of up to two hours.

1 INTRODUCTION

The continually expanding use of Fiber Reinforced Polymer (FRP) composites in large structural applications requires a better understanding of the interdependent thermal and mechanical responses of the FRP when it is subjected to elevated and high temperatures. Thermo-mechanical models using temperature-dependent mechanical properties for FRP materials were developed in the 1980s. In many of the suggested thermo-mechanical models, temperature-dependent E-moduli were developed as stepped functions achieved by connecting experimentally gathered key points, such as the glass transition temperature (T_g) and the decomposition temperature (T_d). E-modulus values at different temperatures were obtained by Dynamic Mechanical Analysis (DMA), as presented, e.g., by Griffis et al. (1986). Mathematical functions were also proposed to describe the change of E-modulus at raised temperatures, such as by Mahieux et al. (2001), by Gibson et al. (2006). By combining the corresponding thermo-chemical model with the mechanical property sub-models, thermal mechanical responses can be predicted, a comprehensive review of these models was reported by Keller et al. (2006a).
In this paper, new temperature-dependent mechanical property models are proposed. Together with these material property sub-models, a thermo-mechanical model is developed to compare predicted and experimental thermal and mechanical responses of three cellular FRP panels subjected to mechanical loads and fire from one side (Keller et al. 2006b). The stiffness degradation and elastic deflections due to thermal loading are described through a temperature-dependent E-modulus sub-model, while the additional deflections due to thermal expansion are considered through a sub-model for the effective coefficient of thermal expansion (CTE). The temperature responses are thereby predicted using the thermal response model developed in Bai et al. (2007a, b).

2 MODELING OF THERMO-MECHANICAL PROPERTIES

2.1 *Temperature-dependent E-modulus*

The thermo-mechanical behavior of FRP composites depends mainly on that of the polymer resin. For the polyester thermosets, four different states (glassy, leathery, rubbery and decomposed) and three transitions (glass transition, leathery-to-rubbery transition, and rubbery-to-decomposed transition) can be defined when the temperature is raised. At each temperature, a composite material can be considered as a mixture of materials in different states, with different mechanical properties. The content of each state varies with temperature, thus the composite material shows temperature-dependent properties. The state changes can be described by the kinetic theory, thus the Arrhenius equations to estimate the quantity of material in each state can be applied. If the quantity of material in each state is known, the mechanical properties of the mixture, E_m, can be estimated over the whole temperature range, as shown in Equation 1:

$$E_m = E_g \cdot (1-\alpha_g) + E_r \cdot \alpha_g \cdot (1-\alpha_d) \tag{1}$$

where E_g is the E-modulus in a glassy state (initial values); E_r is the E-modulus in a rubbery state. Since the E-modules of the leathery and rubbery states are almost the same, the leathery-to-rubbery transition is not necessary to take into account; the material after decomposition is considered without structural stiffness. The quantity of material in each state is determined by the conversion degrees of glass transition and decomposition, α_g and α_d, respectively, which can be calculated based on kinetic theory and Arrhenius equation, as introduced in detail in Bai et al. (2007a, 2008).

Substituting the theoretical results of α_g and α_d into Equation 1, and taking E_g=12.3 GPa as the original modulus, E_r= 3.14 GPa as the modulus at approximately 250°C (modulus of leathery or rubbery state) from DMA experiments (in a three-point-bending configuration within a Rheometrics Solids Analyzer), the temperature-dependent E-modulus can be obtained. A comparison with the DMA data is shown in Figure 1. A good correspondence was found in the temperature range up to 250°C. Furthermore, it can be seen that the second descending stage, resulting from decomposition, can also be captured by the model.

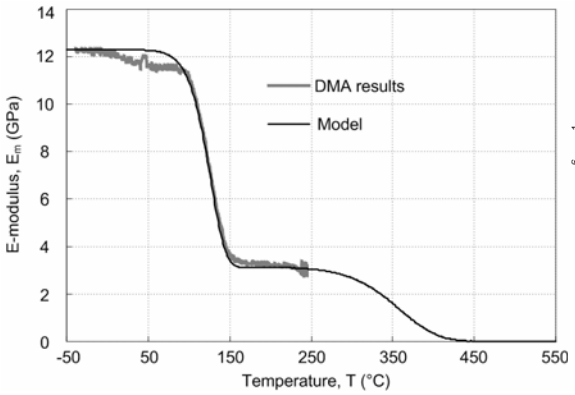

Figure 1. Comparison of E-modulus between model and DMA data.

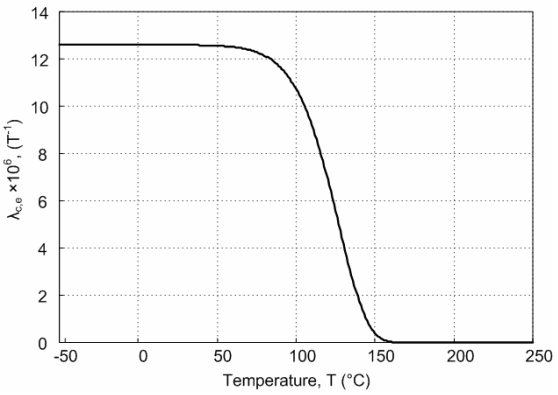

Figure 2. Temperature-dependent effective coefficient of thermal expansion.

2.2 *Temperature-dependent effective coefficient of thermal expansion*

When the temperature is increased, the material in the states after glass transition experiences sudden decreases in the E-modulus and G-modulus, as shown in Figure 1 for the E-modulus. In cross-sections of elements where part of the material remains below the glass transition, the true thermal expansion of the material above the glass transitions does not influence anymore stresses in or deformations of the panel. To consider these structural effects, a concept of an effective coefficient of thermal expansion is proposed. Contributions of the true thermal expansion of the material after glass transition to the global structural deformation are neglected and,

consequently, the effective coefficient of thermal expansion is zero for the material after glass transition. Based on the true coefficient of thermal expansion of the glassy state, λ_c (12.6×10^{-6} K^{-1}, in the longitudinal direction, see Keller et al. 2006a), the temperature-dependent effective coefficient of thermal expansion, $\lambda_{c,e}$, is then expressed as follows:

$$\lambda_{c,e} = \lambda_c \cdot \left(1 - \alpha_g\right) \tag{2}$$

The conversion degree of glass transition, α_g, was obtained from Bai et al. (2008). The resulting temperature-dependent effective coefficient of thermal expansion for the experimental GFRP material is shown in Figure 2.

3 MODELING OF RESPONSES FROM EXPERIMENTS

3.1 *Experimental set-up and results*

Three full-scale specimens (DuraSpan® 766 slab system from Martin Marietta Composites) were fabricated, designated as SLC01, SLC02 and SLC03, with identical configurations and dimensions (see Figure 3). Specimens SLC01 and SLC02 were liquid-cooled during mechanical and thermal loading through slowly circulating water in the cells, while specimen SLC03 was not cooled (Keller et al. 2006b). The specimens were subjected first to serviceability limit state loads (2×92 kN) in a four-point bending configuration. The corresponding pre-fire mid-span deflection was 12.1 mm (average of all specimens).

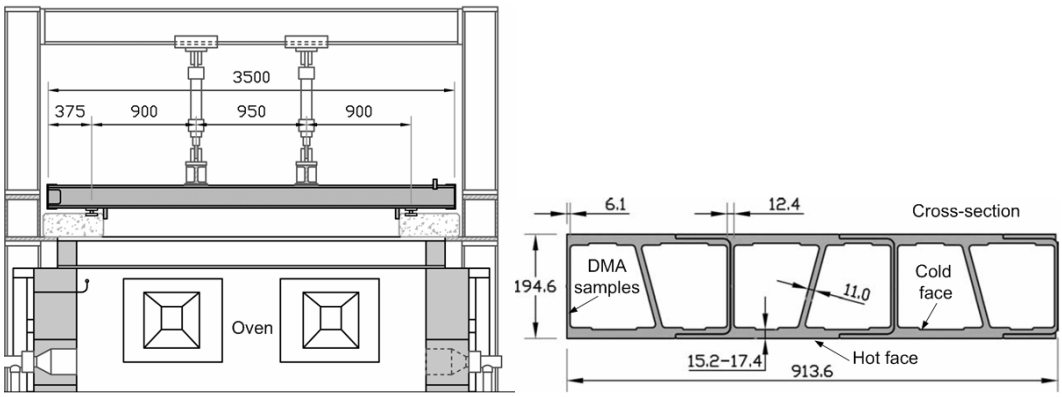

Figure 3. Experimental setup and specimen cross-section for three full-scale GFRP slab specimens.

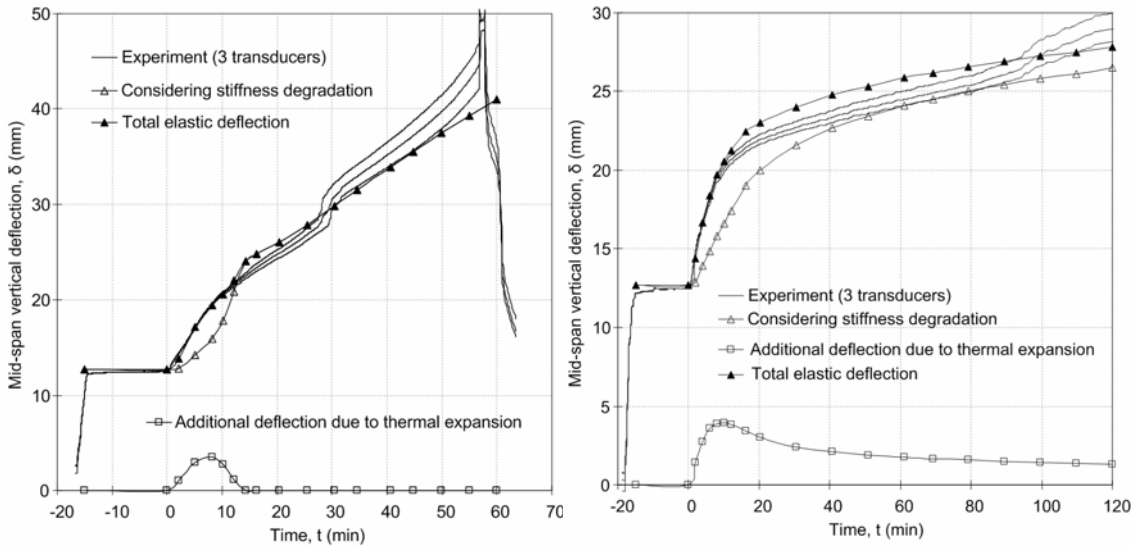

Figure 4. Comparison of deflections from experiments and model for SLC03 (left) and SLC02 (right).

After 15 min., the thermal loading according to the ISO-834 fire curve was applied from the underside. At t=57 min., the non-cooled slab SLC03 failed due to local buckling at the compressed upper face sheet, while the liquid-cooled slabs SLC01/ SLC02 continued sustaining the load up to 90/120 min., when the experiment was stopped. The experimental deflection curves are shown in Figure 4 and will be compared to the corresponding results from thermo-mechanical modeling in the following sections. Due to the similar behavior of specimens SLC01 and SLC02, only results from the latter are referred to in the following.

3.2 *Thermo-chemical model for thermal responses*

Models describing the temperature-dependent thermo-physical properties of FRP composites (density, thermal conductivity, and specific heat capacity) under elevated and high temperatures were proposed in Bai et al. (2007a). By assembling these thermal physical property models, a one-dimensional thermo-chemical model was developed in Bai et al. (2007b) to predict the change of temperature in the lower face sheet of the specimens used in the structural fire endurance experiments. The temperature field obtained from the thermo-chemical model is directly used to calculate the values of α_g and α_d, and the temperature-dependent E-moduli and effective CTE can then be obtained based on Eqs.(1) and (2), respectively.

3.3 *Thermo-mechanical model*

Simplifying the specimen as a simply-supported beam with two point loads, P, Timoshenko beam theory can be used to calculate the elastic deflection at the middle span, δ_E:

$$\delta_E = \frac{aP}{GA}\left(\frac{L-2a}{L}\right)+\frac{PL^3}{24EI}\left(\frac{3a}{L}-\frac{4a^3}{L^3}\right) \tag{3}$$

where L is the span, a is the distance between the load and support, A is the cross-sectional area of the webs, G is the shear modulus, and I is the moment of inertia of the section shown in Figure 3. Since the E-modulus varies over the cross-section during fire exposure, the stiffness of the slab, EI, was calculated as the sum of the stiffnesses of the individual components. Substituting the parameters from Figure 3 into Eq. (3), the initial deflection before thermal loading was calculated as 12.7 mm (105% of experimental value). Of this, 0.61 mm (or 5%) was due to shear deformation and 12.09 mm (95%) was due to bending deformation.

In this specific case, the temperature in the upper face sheet of all specimens remained below the glass transition temperature (SLC03 exhibited the highest temperature: about 75°C after 57 min, which was still below $T_{g,onset}$ = 85°C). Consequently, the E-modulus of the upper face sheet was assumed to remain unchanged in the mechanical model. Similarly, significant temperature changes in the webs were concentrated on the lower part, close to the lower face sheet. Therefore, the E- and G-modulus of the webs were also considered to remain temperature independent.

The lower face sheet of all specimens, however, exhibited steep temperature gradients (see Bai et al. 2007b) and the E-modulus could not be assumed to remain unchanged. By discretizing the lower face sheet into 17 elements in thickness direction (the thickness of one element is almost 1 mm), and the time domain into 60 time steps (thus 1 min. per time step for SLC03 and 2 min. for SLC02), the calculation process for each time step can be summarized as follows:

1. The temperature of each element is calculated by the thermo-chemical model.
2. Based on the available temperature and estimated kinetic parameters, the conversion degrees of glass transition and decomposition are calculated for each element.
3. The E-modulus is estimated from Eq. (1) for each element.
4. The stiffness, EI, of the whole cross section is calculated.
5. Substituting EI obtained at each time step into Eq. (3), the time-dependent mid-span deflection is calculated.

The results of this calculation process are shown in Figure 4 for SLC03 and SLC02, respectively (curves labeled “considering stiffness degradation”).

3.4 *Consideration of effects of thermal expansion*

The deflection curves due to stiffness degradation, shown in Figure 4, persistently underestimate the experimental results, especially at the beginning of the experiments. The underestimation was partially attributed to the non-consideration of thermal expansion. Since only the lower face sheet of the specimens was subjected to thermal loading, the temperature gradient between the upper and lower face sheet induced an additional deflection in the downward direction, which contributed to the increase of total deflection.
The additional deflection, δ_E, due to non-uniform thermal expansion at time step t_i, can be approximately expressed by:

$$\delta_T(t_i) = \frac{\lambda_{c,e}(t_i) \cdot L^2}{8} \cdot \left(\frac{\Delta T}{h} \right)_{t_i} \tag{4}$$

where L is the span of the specimen and $\Delta T/h$ is the temperature gradient through the cross section. $\lambda_{c,e}$ is the time-dependent effective CTE, which was calculated based on Equation 2.

The temperature gradient through the height of the cross section at time step t_i is given by $(\Delta T/h)_{t_i}$. Since the thermal boundary conditions were ambient air for both sides of the upper face sheet and webs, and the ISO fire curve for the hot face of lower face sheet, the measured temperature gradient was highly non-linear along the entire height. In order to apply Eq. (4), the gradient was approximated to be linear. Furthermore, considering that $\lambda_{c,e}$ is not constant along the lower face sheet, an average value of the lower face sheet was adopted at each time step. Based on these approximations, the additional deflections due to thermal expansion were estimated at different time steps and shown in Figure 4.

4 DISCUSSION

A progressive increase in deflection at mid-span of the non-cooled specimen SLC03 can be found in Figure 4 (left). However, when only the stiffness degradation was considered, an underestimation of the measured deflections resulted, especially during the first 15 minutes of thermal loading. The additional deflection due to thermal expansion (Eq. 4), also shown in Figure 4 (left), mainly occurred within the first 15 min. - the period in which the glass transition process in the lower face sheet was not yet finished. After glass transition, the effective coefficient of thermal expansion was set to zero, see Section 2.2. This result explained the discrepancy between the experimental results and the model without taking into account thermal expansion, especially during the first 15 minutes.
Similar to SLC03, the deflection curve of SLC02, resulting from pure stiffness degradation, lays under the experimental deflection curve during the entire fire exposure time, as shown in Figure 4 (right). However, due to the liquid-cooling effects, the conversion degree of glass transition at the cold face of the lower face sheet remained low at 120 min. and, consequently, an additional deflection due to thermal expansion occurred during the duration of the experiment as shown in Figure 4 (right). The total elastic deflection was obtained by summing these two deflection contributors. Compared with the specimen SLC03, the deflection of SLC02 due to stiffness degradation increased much slower and the additional deflection due to thermal expansion lasted longer because of the liquid-cooling effect. In both cases, a good agreement can be found between predicted and measured deflections.

5 CONCLUSIONS

Together with temperature-dependant material property sub-models, a thermo-mechanical model was developed to predict the thermal and mechanical responses (temperature and elastic deflection) of cellular FRP panels subjected to mechanical loads and fire from one side. The results from the model compared well with the results from different full-scale experimental scenarios under realistic fire exposure. The following conclusions were drawn:
1) When subjected to elevated and high temperatures, FRP composites experience complicated

material changes, such as the glass transition and decomposition. As kinetic processes, these transitions can be modeled by the Arrhenius equations, thus the conversion degree of different transitions and the quantity of the material in different states can be obtained.
2) Since the material content of each state is available at any specified temperature, the temperature-dependent mechanical properties, including the E-modulus and the effective CTE, can be determined, for example by a simple mixture approach.
3) Based on the temperature-dependent mechanical properties and on the finite difference method, beam theory then can be used to predict the time-dependent elastic deflections of beam or slab elements subjected to mechanical and thermal loadings for realistic exposure times up to two hours. It was found that during fire exposure the degradation of stiffness and the thermal expansion led to an increase in deflections, while the degradation of stiffness was dominant. Since different thermal boundary conditions can be considered in the model, the benefit of liquid-cooling, which reduces stiffness degradation and increases fire resistance time, could be quantified.

6 REFERENCES

Griffis C.A., Nemes J.A., Stonesfiser F.R., and Chang C.I. 1986. Degradation in strength of laminated composites subjected to intense heating and mechanical loading. J. of Composite Materials, 20, 216-235.

Mahieux C.A., Reifsnider K.L. 2001. Property Modeling across transition temperatures in polymers: a robust stiffness-temperature model. Polymer, 42, 3281-3291.

Gibson A.G., Wu Y.S., Evans J.T. and Mouritz, A.P. 2006. Laminate theory analysis of composites under load in fire. J. Comp. Mater., 40(7), 639-658.

Keller T., Tracy C., Zhou A. 2006a. Structural response of liquid-cooled GFRP slabs subjected to fire, Part II: Thermo-chemical and thermo-mechanical modeling Composites Part A, 37(9), 1296-1308.

Keller T., Tracy C., and Hugi E. 2006b. Fire endurance of loaded and liquid-cooled GFRP slabs for construction. Composites Part A, 37(7), 1055-1067.

Bai Y., Vallée T., Keller T. 2007a. Modeling of thermo-physical properties for FRP composites under elevated and high temperatures. Composites Science and Technology, 67, 3098-3109.

Bai Y., Keller T., Vallée T. 2007b. Modeling of thermal responses for FRP composites under elevated and high temperatures. Composites Science and Technology 67, 3098–3109.

Bai Y, Post NL, Lesko JJ, Keller T. 2008. Experimental investigations on temperature-dependent thermophysical and mechanical properties of pultruded GFRP composites. Thermochim. Acta, doi:10.1016/j.tca.2008.01.002